

Lava-flow characterization at Pisgah volcanic field, California, with multiparameter imaging radar

LISA R. GADDIS *U.S. Geological Survey, 2255 N. Gemini Drive, Flagstaff, Arizona 86001*

ABSTRACT

Multi-incidence-angle (in the 25° to 55° range) radar data acquired by the NASA/JPL Airborne Synthetic Aperture Radar (AIRSAR) at three wavelengths simultaneously and displayed at three polarizations are examined for their utility in characterizing lava flows at Pisgah volcanic field, California. Pisgah lava flows were erupted in three phases; flow textures consist of hummocky pahoehoe, smooth pahoehoe, and aa (with and without thin sedimentary cover). Of the eight AIRSAR images used here, four were calibrated to within an accuracy of ± 2 dB with trihedral corner reflectors, and data from these calibrations were used to process the additional images to a conservatively estimated ± 5 dB level of accuracy. Calibrated radar backscatter data (σ^0 , in dB) were plotted as a function of incidence angle at three wavelengths (P-band, 68 cm; L-band, 24 cm; and C-band, 5.6 cm) and three polarizations (HH, horizontal transmit/horizontal receive; HV, horizontal transmit/vertical receive; and VV, vertical transmit/vertical receive) for eight major units at Pisgah for which multi-incidence-angle AIRSAR data were available. The eight units consist of near-vent and distal aa flows; near-vent and distal, hummocky pahoehoe flows; a mantled, hummocky pahoehoe flow; a platform pahoehoe flow; an alluvial fan; and a playa. Analyses of these backscatter data show that major unmodified volcanic units at Pisgah are readily distinguishable from each other and that they exhibit diffuse (HH, VV) and/or multiple (HV) scattering behavior typical of rough surfaces at these wavelengths. These analyses show that discrimination of smooth lavas (platform pahoehoe) from mantled units with greater primary roughness (hummocky pahoehoe) is difficult and must rely on supporting observations (such as evidence of localized weathering and/or sediment deposition, contrast with surrounding units, and superposition of flow units). L-band back-

scatter and image data at HV polarization show the best discrimination of Pisgah lava flows, with optimal unit separation observed between $\sim 40^\circ$ and 50° incidence angles. Backscatter data shown as a function of relative age of Pisgah flows indicate that dating of lava flows on the basis of average radar backscatter may yield ambiguous results if primary flow textures and modification processes are not well understood.

INTRODUCTION

Recent studies emphasize the importance of understanding the factors governing the appearance of volcanic deposits on radar images (for example, Gaddis and others, 1989, 1990; Mouginis-Mark and others, 1989; Theilig and others, 1989; Gaddis and Greeley, 1990; Head and others, 1991). It has been shown that studies of lava-flow surface textures on radar images are useful for interpretation of flow-emplacment processes and volcanic eruptive histories (Gaddis and others, 1989, 1990). Imaging radar data are expected to be an effective tool for identification and monitoring of potentially dangerous volcanoes in remote areas (Mouginis-Mark and others, 1989). In accordance with petrogenetic arguments suggesting a wide range of possible melt compositions on Venus (Hess and Head, 1990), analyses of Magellan radar data of Venus (Head and others, 1991) show volcanic features consistent with basaltic compositions as well as with more-evolved magmas. In view of the current Magellan radar mission to Venus (Saunders and others, 1990) and the many planned Earth-orbiting radar experiments (for example, Shuttle Imaging Radar-C, Huneycutt, 1989; Earth Observing System, Butler and others, 1987; Radar-sat, Raney, 1984) that will acquire data for a wide variety of volcanic areas, there is a need for (1) geologic analyses of radar signatures of volcanic deposits of diverse morphologies to establish a physical basis for interpretation of radar images, (2) characterization of radar scattering mechanisms for rough surfaces typical of volcanic deposits, and (3) identification of optimal

radar-imaging parameters (wavelength, polarization, incidence angle) for the most effective geologic analyses of volcanic terrains.

This paper presents a study of the effect of varying incidence angle at three wavelengths (P-band, 68 cm; L-band, 24 cm; and C-band, 5.6 cm) and three polarizations (HH, horizontal transmit/horizontal receive; HV, horizontal transmit/vertical receive; and VV, vertical transmit/vertical receive) on characterization of lava-flow surfaces at Pisgah volcanic field, California ($116^\circ 20' W$; $34^\circ 40' N$). Lava flows at Pisgah have textures such as hummocky and smooth ("platform") pahoehoe and aa, with and without thin sedimentary cover (Wise, 1966; Dellwig, 1969). The Pisgah flows erupted from the same vent area and have no major compositional differences (Gawarecki, 1964; Friedman, 1966). Studies of Pisgah with NASA/JPL Airborne Synthetic Aperture Radar (AIRSAR) data allow illustration of the backscatter behavior of lava flows differing largely in surface texture, as well as examination of the effect of mantling by sedimentary deposits on the backscatter behavior of those flows at multiple incidence angles, wavelengths, and polarizations. Objectives of this paper are to (1) illustrate the backscatter behavior of major volcanic units at Pisgah derived from calibrated, multiparameter radar-image data; (2) compare AIRSAR-derived backscatter behavior of Pisgah flows to that observed in previous studies of scatterometer data; and (3) discuss implications of such behavior for interpreting radar images of other volcanic terrains.

Several analyses have used multiparameter radar data to study volcanic deposits (for example, Dellwig and Moore, 1966; Dellwig, 1969; Schaber and others, 1980; Farr and Engheta, 1983; Blom and others, 1987; Blom, 1988; Theilig and others, 1989). Most early studies used uncalibrated radar images in which the intensity of radar return power (or backscatter coefficient, expressed in dB as the radar cross section per unit area, σ^0) from a ground site is measured and displayed so that high returns are bright (for example, as from rough surfaces) and low

returns are dark (for example, as from smooth surfaces). Later studies used calibrated data from a scatterometer, a non-imaging sensor that measures radar backscatter for a site as a function of incidence angle (measured from perpendicular to the surface to the direction of propagation of the transmitted wave). Dellwig and Moore (1966) showed that simultaneously acquired direct- and cross-polarized radar data at K-band wavelengths (~0.8 cm) provide better discrimination of lava-flow boundaries at Pisgah than do direct-polarized data alone. Dellwig (1969) observed wavelength dependence and noted the importance of surface roughness in discriminating Pisgah lava-flow types (aa and pahoehoe) and subsurface features on multi-wavelength (K-band, 0.8 cm; C-band, 7 cm; and P-band, 70 cm) radar images. Schaber and others (1980) showed that long-wavelength (L-band, 25 cm) radar data at direct and crossed polarizations are more useful than short-wavelength (K-band, 0.8 cm; X-band, 3 cm) data for separating volcanic flows at SP Mountain, Arizona, because the flows are uniformly rough at ~3-cm scales. Farr and Engheta (1983), using direct- and cross-polarized scatterometer data of Pisgah at C-band (6 cm) and L-band (19 cm) wavelengths, showed that diffuse, depolarized backscatter is produced from rough aa flows. Blom and others (1987) simulated radar-imaging configurations with scatterometer data of Craters of the Moon, Idaho, and used a statistical approach to select optimal imaging parameters for discrimination of aa and pahoehoe. Blom and others (1987) determined that shorter wavelengths, smaller incidence angles, and horizontally polarized radar data are most useful for studying such lava flows. Blom (1988) compared lava-flow discrimination at different, radar viewing (or "look") directions and showed that for such rough surfaces with no strong directional elements, radar look direction is generally unimportant. Theilig and others (1989) used direct-polarized C-band (6 cm) and L-band (19 cm) scatterometer data of Pisgah to show that mantled pahoehoe is distinctive, but unmantled aa and pahoehoe lava flows cannot be separated readily because their surface roughnesses are too similar at the scale of the radar wavelengths used. Although each of these investigations has yielded important information for the characterization of lava flows at multiple wavelengths, polarizations, and/or incidence angles, none has had the advantage of the unique multiparameter data set provided by the AIRSAR instrument. This paper presents the first analysis of calibrated radar-imaging data, simultaneously acquired at multiple wavelengths and polarizations, for detailed characterization

of lava-flow morphologies at Pisgah volcanic field.

GEOLOGIC SETTING

The Pisgah volcanic field covers ~80 km² and consists of Quaternary basaltic lava flows and a cinder-and-spatter cone superimposed on alluvial and lacustrine sediments (Figs. 1 and 2; Dibblee, 1966; Wise, 1966; Dellwig, 1969). Paleomagnetic data indicate a short eruptive duration (<20 yr) for the entire Pisgah volcanic field (D. Champion, 1990, personal commun., cited in Glazner and others, 1991). Pisgah Crater cone is ~100 m high with a basal diameter of ~500 m. Lava erupted from the cone area in three phases (distinguished by phenocryst textures; Wise, 1966, 1969): Phase I produced pahoehoe; Phase II, aa and pahoehoe; and Phase III, pahoehoe. Field observations show that Phase I pahoehoe lavas are ≤1 m thick, with very smooth, flat surfaces marked by sporadic small ridges (≤5 cm high) or shallow (≤20 cm deep) depressions. To the east, Phase I pahoehoe lavas are extremely smooth ("platform" lava); wind-blown sediments commonly fill shallow depressions. To the west, many Phase I lavas are ridged and may be covered by an eolian and/or alluvial mantle ≤2 m thick. Substantial parts of the Phase I lavas were covered by Phase II aa flows, erupted near Pisgah Crater. To the east, proximal (near-vent) units of Phase II aa lavas are thick (≤5 m), and their very rough surfaces (up to 4 m relief) are characterized by abundant clinker (1- to 20-cm diameter), collapse depressions, and sporadic, rafted pahoehoe plates. To the south, the surface of the distal units of Phase II have a lower relief (<3 m), fewer collapse depressions, and more rafted pahoehoe plates. Northern and western parts of Phase II lavas are thin pahoehoe, with low-relief, ridged surfaces resembling Phase I pahoehoe. During the Phase III eruption, Pisgah Crater cone formed, and the youngest lavas were erupted to the south and east. Phase III pahoehoe lavas are thick (~3 to 5 m), characterized by hummocky surfaces with pressure ridges and tumuli ≤3 m high. At the south edge of Pisgah, Phase III pahoehoe is covered by up to 3 m of alluvium, but in the west-central part of the Phase III lavas, streaks and pockets (≤1 m deep) of wind-blown sediments are common.

Southeast of Pisgah volcanic field lies the Lavic Lake playa (~3 km across), composed of hard, generally dry, argillic materials (Wise, 1966). The surface of Lavic playa is extremely flat and has numerous desiccation polygons as much as 10 m across. Flows erupted from a smaller cinder cone, Sunshine Crater, are found

to the southwest of Pisgah and Lavic. The north and southwest edges of Lavic playa are covered by Pisgah and Sunshine flows, respectively; to the south and east, it is bordered by alluvial fans. At the north edge of the playa, cobbles of Phase I lava are detached and loosely distributed across the playa surface.

DATA

Multiparameter radar data used in this study were acquired June 3, 1988, by AIRSAR during the Mojave Field Experiment (Wall and others, 1988) over Pisgah volcanic field (Fig. 3). These radar data were processed to a pixel size of 10 × 10 m and were acquired at 3 wavelengths simultaneously. Although any combination of transmitted and received polarizations may be simulated by using the complete polarimetric capabilities of the instrument (Zebker and others, 1987; van Zyl and others, 1987), in order to provide direct comparisons with data to be acquired by systems such as Magellan, SIR-C, and EOS, only direct- and cross-polarized data (HH, HV, VV) were used in this analysis. Multi-incidence angle data for a site were acquired by moving the AIRSAR ground swath. In each image, incidence angle varies from ~25° in the near range to ~55° in the far range of the ground swath. In all, eight images of parts of the Pisgah volcanic field were obtained.

AIRSAR data are calibrated through analysis of the backscatter from trihedral corner reflectors (van Zyl, 1990). Trihedral reflectors (6 ft, 1.8 m) were deployed at ~2-km spacing on the smooth surface of Lavic Lake playa; 5 reflectors spanned the width of the 10-km ground swath. After standard phase calibration and cross-talk removal, channel imbalance correction and absolute radiometric calibration were conducted by matching the polarization signatures of the observed reflectors and an ideal trihedral reflector (van Zyl, 1990), permitting calculation of backscatter coefficients for units within calibrated images. Calibrated backscatter coefficients (expressed as σ^0 in dB, or radar cross section per unit area) are quantitative measures of radar return power integrated over a unit area. These calibration techniques are most applicable to radar scenes with corner reflectors, but due to the extreme stability of the AIRSAR system, they may be extended reasonably to adjacent frames along the same track (Freeman and others, 1989). Of the eight AIRSAR images of Pisgah, four include corner reflectors or are adjacent to images with reflectors and were calibrated to within an estimated accuracy of ±2 dB (Freeman and others, 1989; van Zyl, 1990). Further extension of these techniques to images

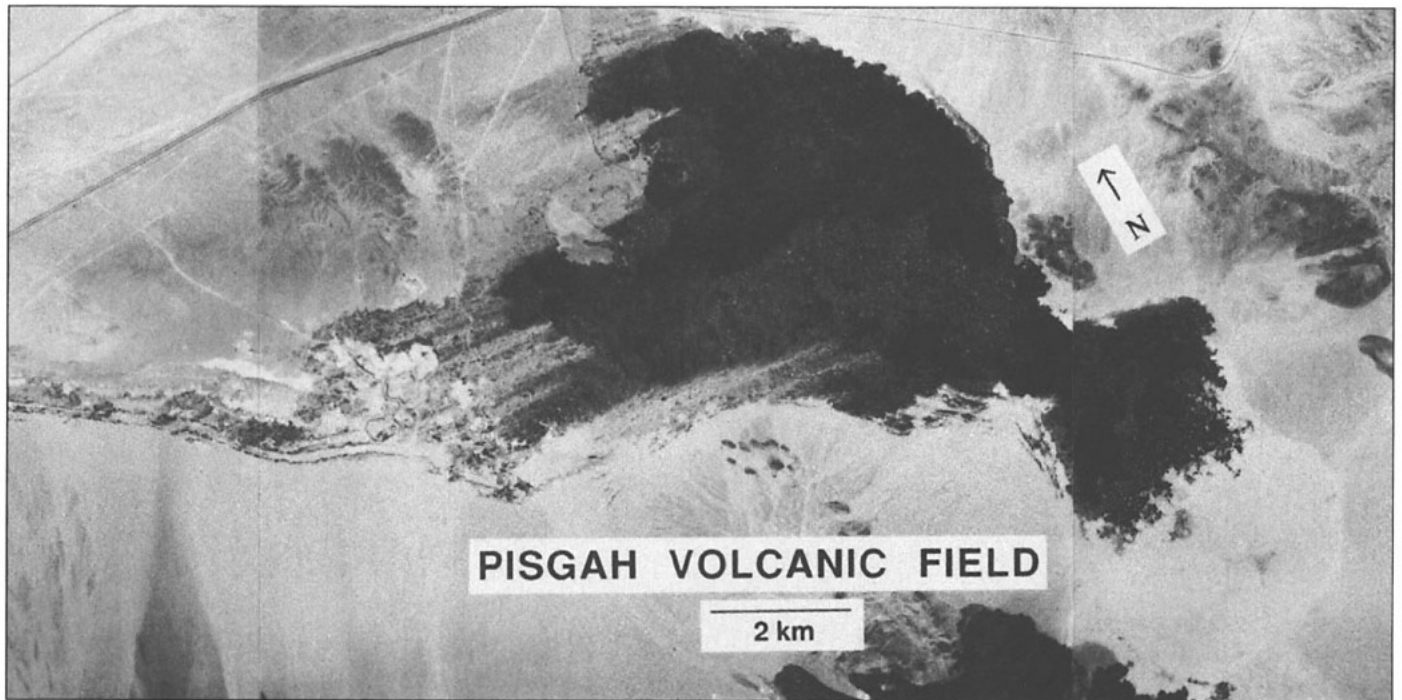


Figure 1. Airphoto of Pisgah volcanic field (June 1988).

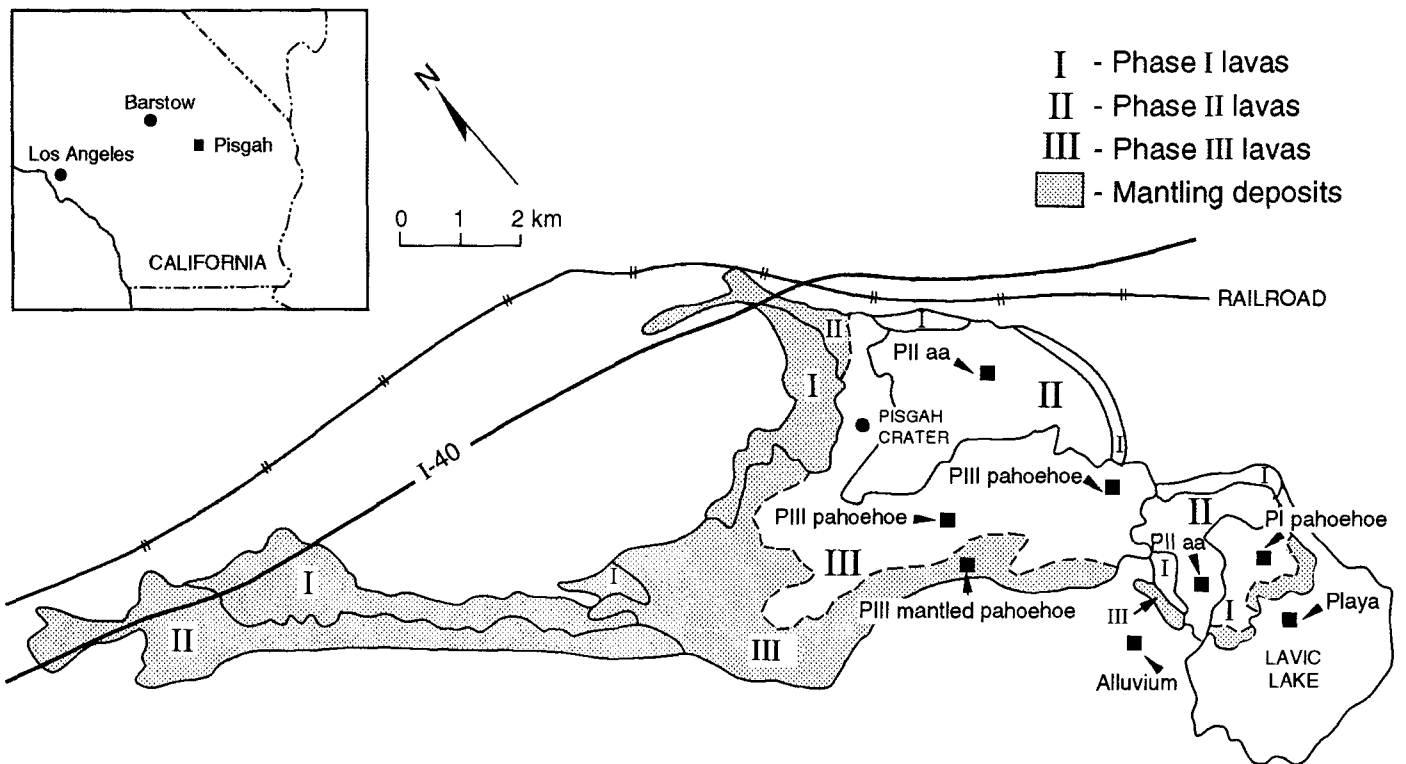


Figure 2. Geologic sketch map of Pisgah volcanic field showing major geologic units and the eight sites (squares) from which σ^o values were extracted.

PISGAH VOLCANIC FIELD

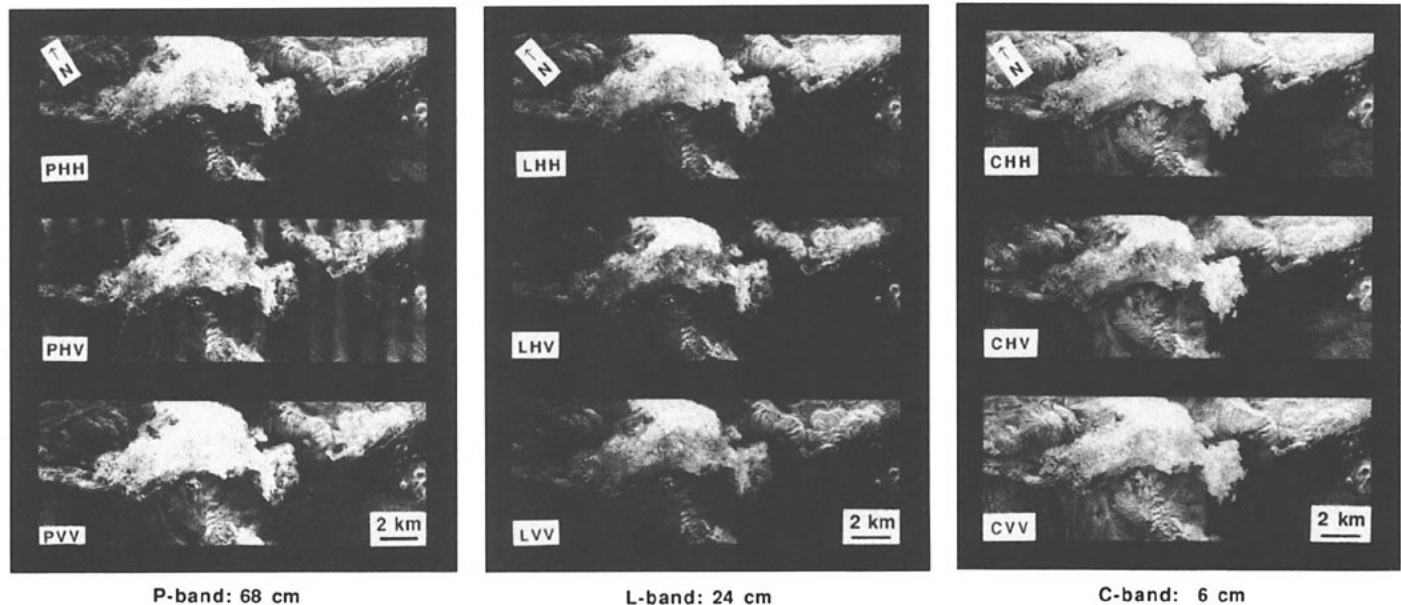


Figure 3. Slant-range AIRSAR image of Pisgah volcanic field shown at three wavelengths and three polarizations. The radar look direction is from top to bottom, the incidence angle ranges from $\sim 25^\circ$ to 55° from near- (top) to far-range (bottom), and the pixel size is $\sim 10 \times 10$ m.

acquired for the same area at different times along different flight paths (for example, data subject to variations in aircraft and instrument parameters such as altitude and antenna gain) has permitted processing of the remaining four Pisgah images to within a conservatively estimated ± 5 dB level of accuracy (A. Freeman, 1991, personal commun.). From the calibrated data, backscatter coefficients were calculated at P-, L-, and C-band wavelengths and at HH, HV, and VV polarizations for eight sites at Pisgah (Fig. 2). Because of overlapping coverage at Pisgah, the number of incidence angles for each of the eight sites ranges from four to six.

Radar backscatter is a function of target properties (approximately wavelength-scale surface and/or subsurface roughness, topographic slope, dielectric constant) and instrument parameters (wavelength, polarization, look angle, incidence angle, look direction). For dry, unvegetated, low-relief geologic units with few compositional differences such as those at Pisgah volcanic field, surface roughness at approximately the scale of the radar wavelength has the dominant effect on radar backscatter at incidence angles $\geq 20^\circ$ (for example, Ulaby and others, 1982; Farr and Engheta, 1983; Gaddis and others, 1989). At a given incidence angle (θ) and

radar wavelength (λ), the amount of scattering from a slightly rough surface is proportional to the amplitude of the roughness spectral component that satisfies the Bragg scattering condition, $\Lambda = \lambda/2\sin\theta$ (Valenzuela, 1967). In simple terms, direct-polarized radar data are most sensitive to a single scale of roughness of scatterers, whereas cross-polarized data respond to the average geometry or texture of scatterers (for example, Daily and others, 1978). It is therefore expected that surfaces with a small amount or amplitude of wavelength-scale roughness elements will show low backscatter, and those with a large amount or amplitude of wavelength-scale roughness elements will show high backscatter.

The behavior of σ° as influenced by incidence angle, polarization, and wavelength is illustrated in Figure 4, which shows the variation in σ° for different surface roughnesses (where roughness is relative to a given radar wavelength; Fig. 4a) and at different polarizations (Fig. 4b; Ulaby and others, 1982). In Figure 4a, a typical direct-polarized backscatter curve for a slightly rough surface shows a moderate negative slope with two parts, a quasi-specular ("coherent") component at small incidence angles ($< 20^\circ$) and a diffuse ("noncoherent") component at larger in-

cidence angles ($> 20^\circ$). As surface roughness increases, the curve slope becomes less negative and is dominated by the diffuse component of backscatter. For a very rough surface, the backscatter curve is least sensitive to incidence angle and is relatively flat. For a rough surface at incidence angles greater than $\sim 30^\circ$, backscatter is largest at vertical polarization, intermediate at horizontal polarization, and smallest at crossed polarizations (Fig. 4b). Direct-polarized backscatter is due to single scattering (either quasi-specular or diffuse) from surface or subsurface features, and cross-polarized backscatter is a result of multiple scattering on or beneath a surface (Fung and Eom, 1979).

RADAR DATA ANALYSIS

Backscatter curves at three wavelengths and three polarizations for eight sites at Pisgah (Fig. 5) are shown in Figure 5. Of the eight sites, six are volcanic units (rough to smooth); data from two smoother sites (one alluvial fan, one playa) are shown for comparison. Note that, as expected for decreasing roughness, the slope of each series of backscatter curves ranges from approximately flat (a, b) to slightly negative (c, d, e, f) to negative (g, h). Backscatter curves

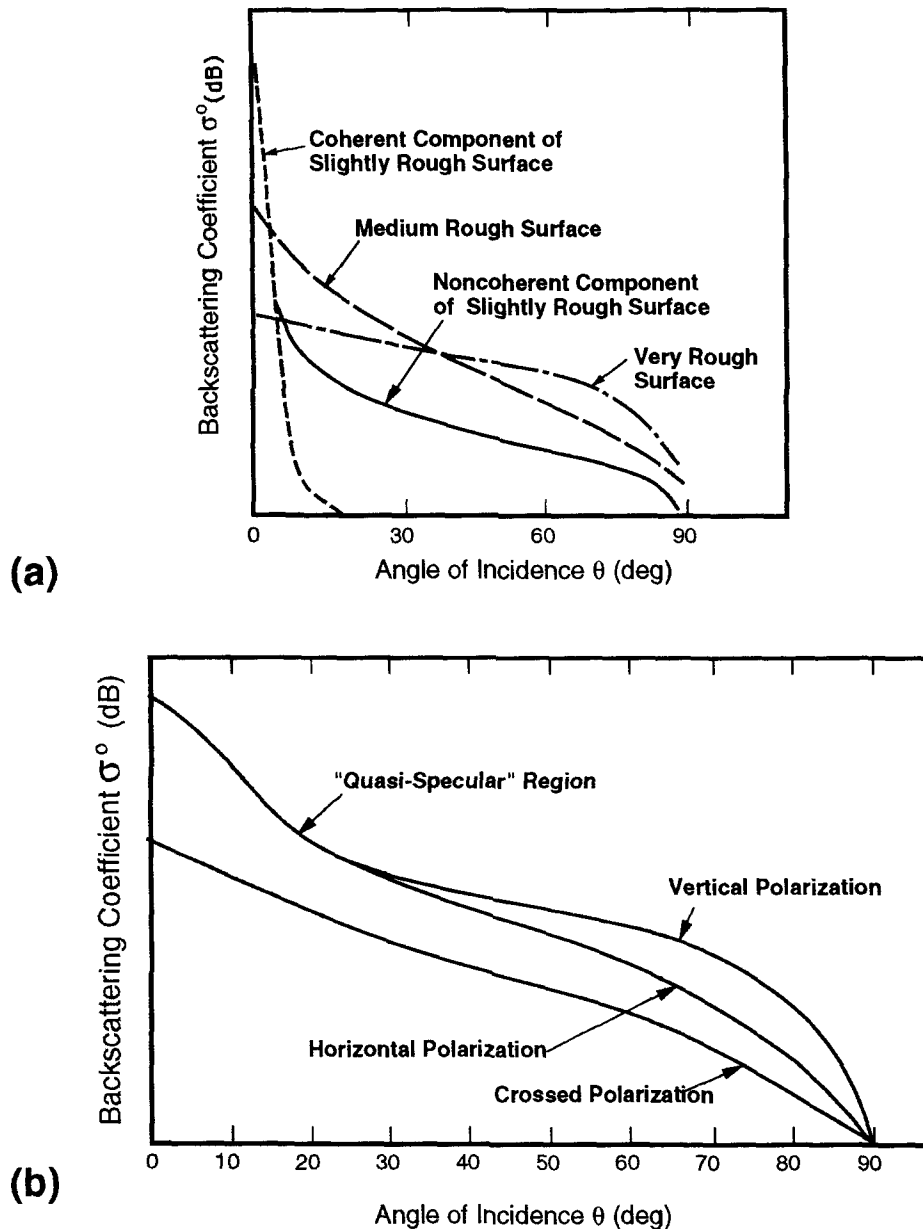


Figure 4. Generalized radar backscatter curves for surfaces (a) of differing roughness and (b) at different polarizations (after Ulaby and others, 1982).

for these eight units at Pisgah thus behave as "very rough" and "medium rough" surfaces according to conceptual backscatter relations (Fig. 5). With decreasing surface roughness, the average σ^0 decreases, and the range (for example, the separation among individual curves) increases for each set of curves. These trends indicate that wavelength and polarization are important factors for unit discrimination among smoother units at Pisgah. As expected, in each case direct-

polarized data have higher average σ^0 than cross-polarized data (the vertically polarized data are slightly higher on average than the horizontally polarized data). Separation among wavelengths is greatest at cross-polarizations in all cases, which indicates that cross-polarized data can provide a useful addition to direct-polarized data and may be superior for volcanic unit discrimination at Pisgah. Cross-polarized backscatter provides evidence for

multiple scattering (Fung and Eom, 1979) and this, in combination with the enhanced discrimination of lava flows at cross-polarizations, suggests that the Pisgah volcanic units are more distinctive in their average roughnesses or surface textures than in their specific wavelength-scale roughnesses. Note that in most cases, the greatest separation among these backscatter curves is observed between $\sim 40^\circ$ and 50° angles of incidence, which suggests that the best discrimination among Pisgah volcanic units on the basis of surface texture is expected in this range of incidence angles. Within each polarization grouping, furthermore, the average σ^0 decreases as wavelength increases (for example, CVV is commonly highest, followed by LVV, then PVV, etc.). These data confirm expectations that rougher volcanic surfaces produce higher average radar returns and that such units are less sensitive to variations in incidence angle, wavelength, and polarization than are smooth surfaces.

For a more detailed analysis of lava-flow characterization at different incidence angles and polarizations, the L-band data are emphasized, because more lava-flow textures are observed on those image data (Fig. 3). Apparently, most geologic surfaces near Pisgah are almost uniformly rough at C-band wavelengths (~ 6 cm), and so little discrimination among units is possible on these data. At P-band wavelengths, fewer volcanic units are distinctive at a 70-cm scale of roughness and average texture, whereas at the 25-cm scale of the L-band data, many of the known lava-flow textural types at Pisgah produce different amounts of backscatter. Figure 6 shows L-band backscatter curves at HH, HV, and VV polarizations for the eight units in this study. Note that the overall separation among backscatter curves is greatest for the cross-polarized data (Fig. 6b), which again suggests that such data may be most useful for discrimination of these "medium rough to very rough" lava flows on the basis of different amounts of multiple scatter caused by different surface textures or average roughnesses. Among the backscatter curves at all three polarizations, those of the two aa units (near-vent and distal) are very similar and have distinctly higher backscatter than other volcanic units (particularly at LHV; Fig. 6b). Although the two Phase III hummocky pahoehoe units (central and eastern) have intermediate radar returns and are separable on the L-band radar images (Fig. 3), the backscatter curves for these units are very similar at all polarizations (Fig. 6). It seems that the spatial variations in image tone are more distinctive for the

two Phase III hummocky pahoehoe units than are the point measurements of backscatter shown in Figure 6. The backscatter curve for Phase III mantled pahoehoe, however, is distinguishable clearly from both of the higher-return units of Phase III unmantled hummocky pahoehoe at each polarization (Fig. 7). The backscatter data for Phase III mantled pahoehoe, although slightly higher return, overlap those of Phase I platform pahoehoe at $\sim 40^\circ$ incidence angle. Apparently the smoothing effects of the mantling deposits inhibit clear separation of the youngest, Phase III mantled pahoehoe and the oldest, intrinsically smoother, Phase I platform pahoehoe. All of the volcanic units in this study have higher radar returns and are distinguishable from the low-return, smooth alluvial fan and playa units at L-band wavelength scales (Figs. 3 and 6). Again, these curves (Fig. 6) show that the greatest degree of separation, and thus the best unit discrimination, is observed at $\sim 40^\circ$ to 50° incidence angles.

DISCUSSION

Several important observations can be made from backscatter data from Pisgah volcanic field. In part because of the incidence-angle range of the AIRSAR data ($\sim 25^\circ$ – 55°), backscatter curves primarily show diffuse (for HH and VV data) and/or multiple (for HV data) scattering for all volcanic units in this study. As compared to the schematic backscatter curves of Figure 4, all of the backscatter curves for Pisgah (Fig. 5) show scattering behaviors typical of very rough surfaces. Zebker and others (1987) have indicated that a first-order Bragg scattering model does not account adequately for the scattering behavior of very rough surfaces typical of lava flows. These backscatter curves show that only mantled (Fig. 6e) and platform pahoehoe (Fig. 6f) might generously be considered to produce backscatter curves of radar-smooth surfaces and thus to be suitable for modeling as Bragg-like surfaces. In addition, different textural types of unmantled aa and pahoehoe are not distinctive in their backscatter signatures; surface textural distinctions that can be made in the field among these rough units (such as proximal and distal aa) cannot be clearly deduced from backscatter curves. These curves thus allow comparison with theoretical models and discrimination of types of scattering, but the radar images show spatial and image textural relations (and enhanced unit discrimination) that are difficult to recognize in the curves. For example, although enhanced unit discrimination at cross polarizations is observed on the radar images (Fig. 3), such an enhancement is only suggested by the curves (Figs. 5 and 6). The use of both radar-

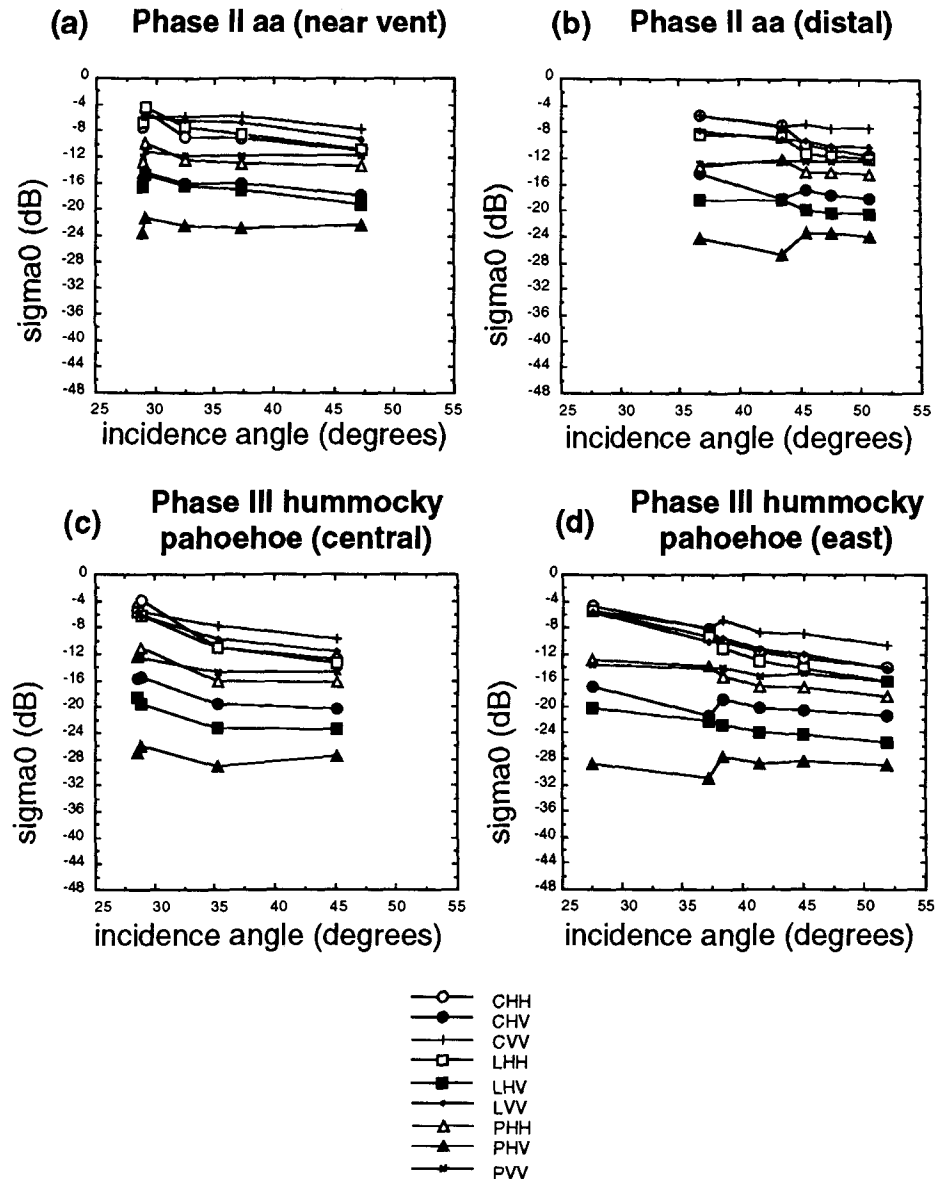


Figure 5. Calibrated radar backscatter curves for eight major units at Pisgah in order of decreasing roughness. Curves are shown for horizontally (HH), cross-polarized (HV), and vertically (VV) polarized data at C- (5.6 cm), L- (24 cm), and P-band (68 cm) wavelengths.

image and quantitative-backscatter data is warranted for the most effective geologic interpretation of volcanic terrains. The radar images also provide the best wavelength comparisons: at C-band, most volcanic units are high return and thus radar rough at 6-cm scales; at P-band, more backscatter or image-brightness differences among the lava flows are observed, but many units are similar at 70-cm scales; at the 25-cm L-band scale of roughness and average surface texture, units are more distinctive and thus brightness differences among them are distinctive, especially at crossed polarization (LHV). These observations indicate that LHV image

data, responsive to surface structure or average texture at ~ 25 -cm scales, are the most useful for characterization of the lava flows at Pisgah. Further work with radar data of other, texturally different, volcanic terrains is necessary to determine whether this result is general or applicable only to the Pisgah volcanic field and these AIRSAR data.

These observations of multiparameter backscatter relations among different lava-flow units at Pisgah volcanic field support many of the interpretations of previous workers. Simultaneously acquired multipolarization and multi-wavelength radar data remove the temporal

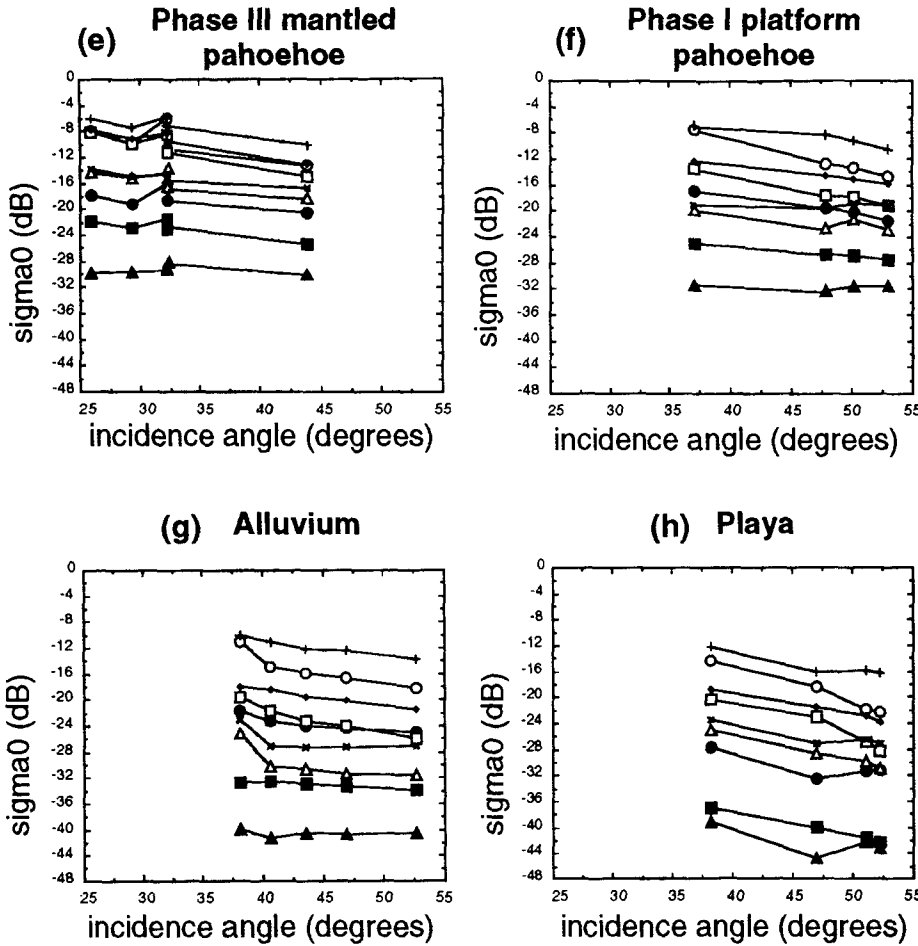


Figure 5. (Continued).

differences that may cause problems in interpretation of data acquired at different times (Dellwig and Moore, 1966). Combined direct- and cross-polarized radar data provide enhanced lava-flow discrimination (Dellwig and Moore, 1966; Dellwig, 1969); longer-wavelength data such as L-band data are more useful for studies of volcanic deposits, because such rough surfaces appear almost uniformly high return at shorter wavelengths (Schaber and others, 1980; Farr and Engheta, 1983; Theilig and others, 1989). In contrast to the conclusion of Blom and others (1987) that shorter wavelengths, smaller incidence angles, and horizontally polarized data are best for lava-flow discrimination, the backscatter data presented here indicate that longer wavelengths, larger incidence angles, and cross-polarized data are most useful for separation of lava flows at Pisgah. It should be noted that if incidence angles below $\sim 25^\circ$ are removed from consideration in the statistical selection of synthesized imaging-radar configurations of Blom and others (1987), longer wavelength, cross-polarized data would be more significant in their results. Unlike the result of Theilig and others (1989) that Phase II aa and Phase III unmantled pahoehoe are difficult to separate in CHH and LHH scatterometer data, backscatter data presented here (Fig. 7) show clear separation of the Phase II aa and Phase III pahoehoe at all three polarizations, particularly LHV.

It is difficult to compare the scatterometer data of Blom and others (1987) and Theilig and others (1989) with backscatter data presented here for several reasons. Backscatter data at

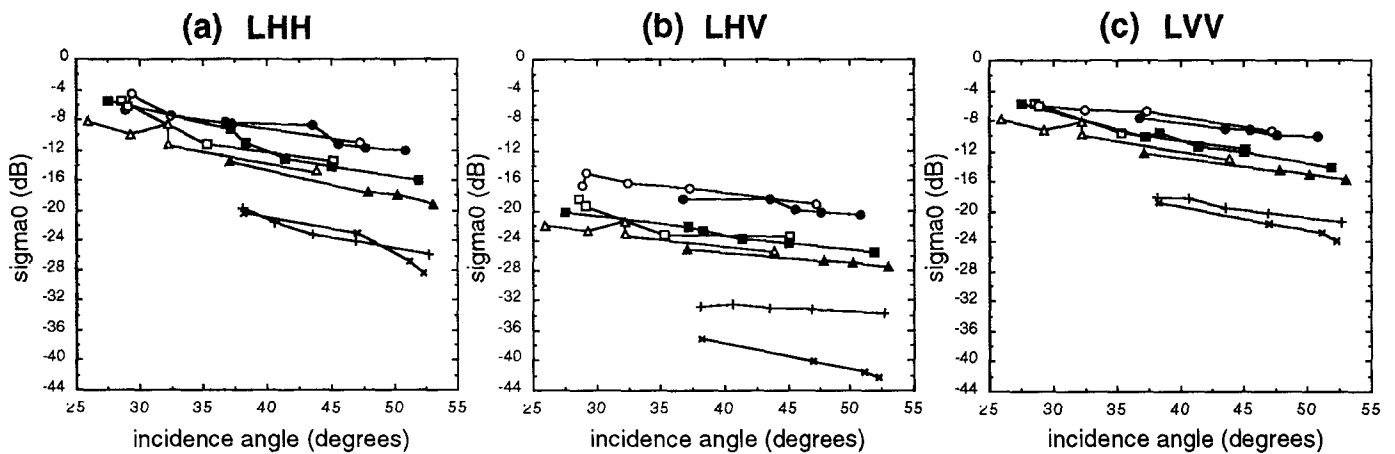


Figure 6. L-band (24 cm) radar backscatter curves for same eight PIsagah units as in Figure 5: (a) HH, (b) HV, and (c) VV.

- aa (near vent)
- aa (distal)
- ph3 pah (cent)
- ph3 pah (east)
- △ ph3 mant pah
- ▲ ph1 pah
- alluvium
- + playa

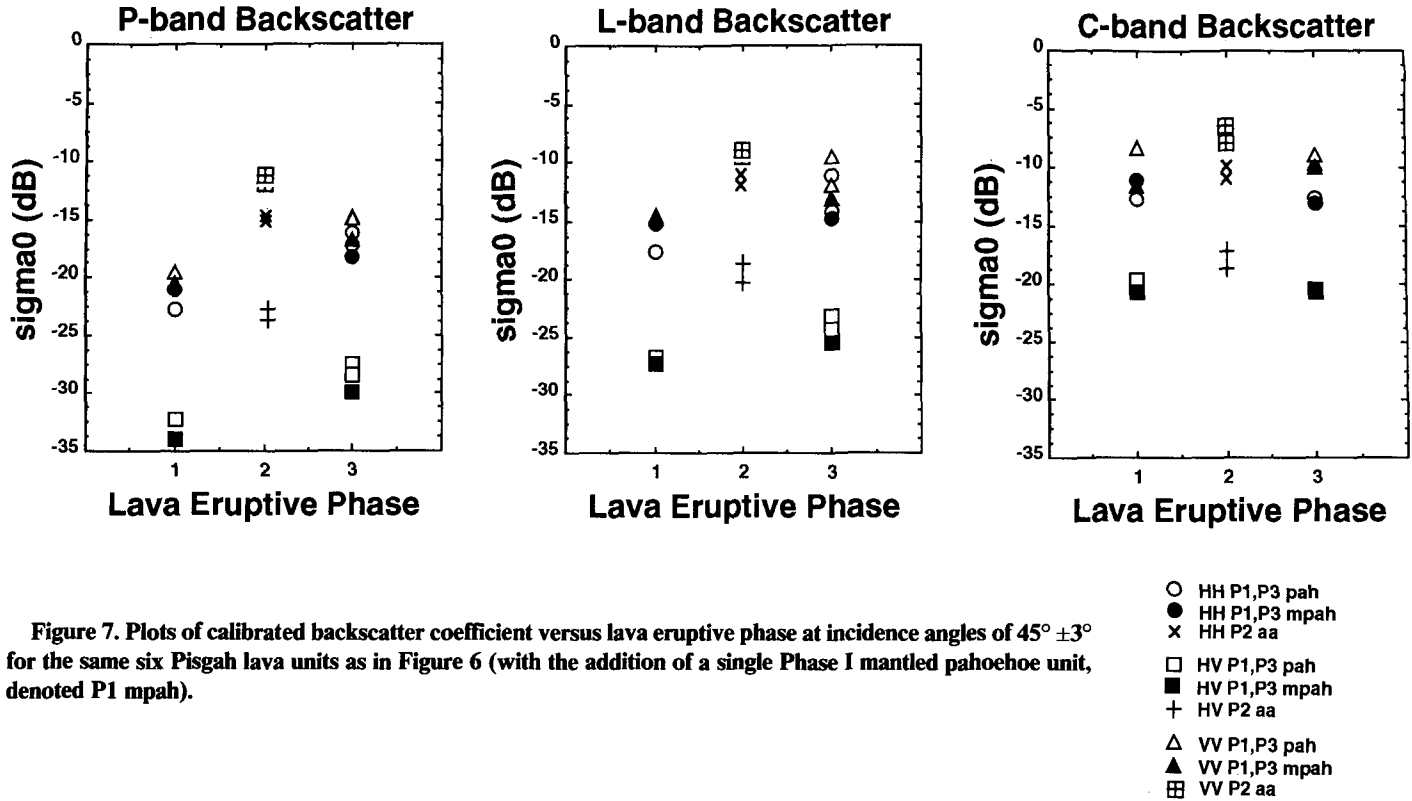


Figure 7. Plots of calibrated backscatter coefficient versus lava eruptive phase at incidence angles of $45^\circ \pm 3^\circ$ for the same six Pisgah lava units as in Figure 6 (with the addition of a single Phase I mantled pahoehoe unit, denoted P1 mpah).

smaller incidence angles ($<20^\circ$) were prominent in their analyses of scatterometer data. Lava flows at Craters of the Moon (Blom and others, 1987) may not be texturally comparable with those at Pisgah, and only "typical" aa, pahoehoe (Phase III hummocky pahoehoe), and mantled pahoehoe (actually a Phase I mantled pahoehoe unit) were used in the Theilig and others (1989) analysis.

The availability of these calibrated data and the strong dependence of radar backscatter on surface roughness suggest that radar might be a useful tool for estimating lava-flow ages (for example, Farr, 1985; Blom and others, 1986). Although with only three eruptive phases of unknown ages, the Pisgah data are not the best to use for such a demonstration, they do permit statements to be made about the use of radar data for the relative dating of flows. First, it is expected that lava-flow roughness and thus radar brightness decreases as a flow ages, so, in the Figure 7 plot of backscatter versus flow eruptive phase at three wavelengths, positive slopes are anticipated and are observed at P- and L-bands. At C-band in Figure 7, the distribution of data for all lava phases is approximately flat, in accordance with the nearly uniform roughness of these deposits at 6-cm scales of roughness. Regardless of relative age, however, aa is intrinsically rougher (and thus higher return) than pahoehoe, and a rise corresponding to the

Phase II aa is observed in each distribution in Figure 7. This rise might be disregarded on the basis of our knowledge of the flow textures present at Pisgah, but, as observed in Figure 3, it is not always obvious on radar images which is aa and which is pahoehoe. Phase I pahoehoe flows are observed to be smoother than those of Phase III (for example, Wise, 1966). This difference can be seen at P- and L-band wavelengths in Figure 7, where data for unmantled Phase I pahoehoe (open symbols) closely overlap those for mantled Phase I pahoehoe (filled symbols) ($\Delta\sigma^{\circ}_{Phh} = 1.7$ dB; $\Delta\sigma^{\circ}_{Phv} = 1.7$ dB; $\Delta\sigma^{\circ}_{Pvv} = 0.9$ dB; $\Delta\sigma^{\circ}_{Lhh} = 2.4$ dB; $\Delta\sigma^{\circ}_{Lhv} = 0.6$ dB; $\Delta\sigma^{\circ}_{Lvv} = 0.2$ dB), particularly at VV polarizations (where response to vertically oriented scatterers is likely to be highest). In the case of P- and L-band responses to Phase III lavas, the two unmantled pahoehoe units (open symbols) and one mantled pahoehoe unit (filled symbols) are clearly distinguishable at both HH and VV polarizations ($\Delta\sigma^{\circ}_{Phh} = 2.0$ dB; $\Delta\sigma^{\circ}_{Phv} = 2.5$ dB; $\Delta\sigma^{\circ}_{Pvv} = 2.0$ dB; $\Delta\sigma^{\circ}_{Lhh} = 3.7$ dB; $\Delta\sigma^{\circ}_{Lhv} = 2.3$ dB; $\Delta\sigma^{\circ}_{Lvv} = 3.5$ dB). Note that, as observed in Figure 5, average backscatter for the unmantled Phase I pahoehoe is closest to that of the mantled Phase III pahoehoe. Because Phase I pahoehoe is intrinsically smoother than Phase III pahoehoe, it is expected that less mantling material would be required to smooth out its surface. These backscatter relations among

known Pisgah flow textures indicate that the use of radar data for estimating lava-flow ages requires two assumptions: that primary flow textures are very similar and that modification processes act uniformly. Thus radar backscatter data can best be used for lava-flow age characterization where primary textures and modification processes are well understood.

CONCLUSIONS

The following conclusions can be derived from these detailed analyses of radar backscatter relations among lava flows at Pisgah volcanic field. At all wavelengths and polarizations, the roughest units (Phase II aa flows) are clearly higher return than, and can be distinguished readily from, all other geologic units within the study area. Hummocky (Phase III) pahoehoe flows are also clearly identifiable as separate units on the basis of their intermediate radar returns. Accurate discrimination, however, of very smooth lava surfaces (such as the Phase I platform pahoehoe) from surfaces of greater primary roughness that have been modified (such as the Phase III mantled pahoehoe) is difficult; it must rely on supporting observations such as evidence of localized weathering and/or sediment deposition, contrast with surrounding units, and superposition of flow units.

The backscatter curves (with $\sim 25^\circ$ – 55° inci-

dence angles) presented for most Pisgah lava flows (Figs. 5 and 6) show diffuse and/or multiple scattering behavior typical of "very rough" surfaces (Fig. 4a). Only mantled (Fig. 6e) and platform pahoehoe (Fig. 6f) units exhibit backscattering behavior that might be considered typical of "medium rough" or "slightly rough" surfaces (Fig. 4a). Roughness measurements (surface-height standard deviations, or "rms heights") for Pisgah lava flows include values of 6.5–7.5 cm for Phase III mantled pahoehoe (Wall and others, 1991), 13.8 cm for Phase II aa, 3.0 cm for Phase I mantled platform pahoehoe (S. Wall, 1989, personal commun.), and 2.9 cm for Phase I platform pahoehoe (van Zyl and others, 1991). These backscatter curves and roughness data suggest that simple scattering models (for example, Bragg scattering, small perturbation model; Ulaby and others, 1982) that are applicable to "slightly rough" surfaces (for example, approximately flat surfaces with rms heights <5% of the radar wavelength, or <3.4 cm for P-band, <1.2 cm for L-band, and <0.3 cm for C-band) are not appropriate for application to many lava flows. This observation is supported by results of Zebker and others (1987) who showed that a first-order Bragg scattering model does not account adequately for the scattering behavior of the very rough surfaces typical of lava flows. Results of van Zyl and others (1991) also indicate that only the Phase I platform pahoehoe is smooth enough among lava flows at Pisgah to warrant application of the small-perturbation scattering model. Empirical roughness versus scattering relations derived from data such as these calibrated AIRSAR data might be most appropriate for derivation of scattering properties of volcanic terrains.

On the basis of image and backscatter relations, discrimination among texturally distinct volcanic units at Pisgah is best at L-band wavelengths and cross-polarization, and incidence-angle variation is the least influential parameter. Smoother surfaces (mantled pahoehoe and platform pahoehoe), however, show a greater dependence on incidence-angle variation than do rougher surfaces. For distinguishing volcanic units at Pisgah, L-band is the best overall wavelength, cross-polarized data show the best surface textural discrimination, and incidence angles from ~40° to 50° are optimal. Although an appropriate scattering model for most lava flow surfaces has not been identified, these results indicate that scattering in the 40° to 50° incidence-angle range produces radar signatures that are most distinctive for lava-flow surfaces with average roughnesses or textures in the 25-cm (L-band) wavelength size range.

Although it is reasonable to postulate that average flow brightness decreases with flow age, the extreme brightness of the Phase II aa flow at Pisgah can be assumed to be related to a primary-emplacment texture that is intrinsically rougher than the surrounding intermediate-return units. Thus the age of the aa unit, apparently younger strictly on the basis of average radar backscatter, is actually indeterminate on the basis of these radar data. Likewise, the oldest Phase I platform pahoehoe is difficult to distinguish from the youngest mantled Phase III hummocky pahoehoe. The use of average backscatter alone for relative lava-flow dating may yield ambiguous results if primary flow textures and modification processes are not well understood.

These results provide important constraints on the selection of optimal radar-imaging parameters for the geologic characterization of volcanoes (for example, Magellan and the planned NASA SIR-C and EOS missions). Furthermore, the backscatter data presented here may provide guidelines for the identification of a variety of lava-flow textures and the subsequent interpretation of eruptive histories of volcanic terrains on Earth as well as on other planets such as Venus.

ACKNOWLEDGMENTS

I acknowledge with gratitude generous assistance with data and software for AIRSAR image calibration and analysis from Jakob van Zyl; Howard Zebker; Fred Burnette; Diane Evans; Tom Farr and other members of the Jet Propulsion Laboratory Radar Sciences Group; numerous members of research teams from Arizona State University, Washington University, and the Jet Propulsion Laboratory, who provided field work during the Mojave Field Experiment spearheaded by Steve Wall. I am also pleased to acknowledge the careful, thoughtful reviews by Tom Farr and an anonymous reviewer.

REFERENCES CITED

- Blom, R. G., 1988, Effects of variation in look angle and wavelength in radar images of volcanic and aeolian terrains; or Now you see it, now you don't: *International Journal of Remote Sensing*, v. 9, p. 945–965.
- Blom, R. G., Cooley, P., and Schenck, L. R., 1986, On the relationship between age of lava flows and radar backscatter: *International Geoscience and Remote Sensing Symposium*, Zurich, Proceedings, p. 1119–1127.
- Blom, R. G., Schenck, L. R., and Alley, R. E., 1987, What are the best radar wavelengths, incidence angles, and polarizations for discrimination among lava flows and sedimentary rocks? A statistical approach: *IEEE Transactions on Geoscience and Remote Sensing*, v. GE-25, p. 208–213.
- Butler, D. M., Gurney, R. J., and Miller, T. L., 1987, EOS: The Earth observing system and polar platforms: *Eos (American Geophysical Union Transactions)*, v. 68, p. 1579–1586.
- Daily, M., Elachi, C., Farr, T., and Schaber, G., 1978, Discrimination of geologic units in Death Valley using dual frequency and polarization imaging radar data: *Geophysical Research Letters*, v. 5, p. 889–892.
- Dellwig, L. F., 1969, An evaluation of multifrequency radar imagery of the Pisgah Crater area, California: *Modern Geology*, v. 1, p. 65–73.
- Dellwig, L. F., and Moore, R. K., 1966, The geological value of simultaneously produced like- and cross-polarized radar imagery: *Journal of Geophysical Research*, v. 71, p. 3597–3601.
- Dibblee, T. W., 1966, Geologic map of the Lavic quadrangle, San Bernardino County, California: *U.S. Geological Survey Map 1-472*, scale 1:62,500.
- Farr, T. G., 1985, Age-dating volcanic and alluvial surfaces with multipolarization data: *NASA/JPL Aircraft SAR Workshop Proceedings*, Jet Propulsion Laboratory Publication 85-39, p. 31–36.
- Farr, T. G., and Engelta, N., 1983, Quantitative comparisons of radar image, scatterometer, and surface roughness data from Pisgah Crater, CA: *International Geoscience and Remote Sensing Symposium*, San Francisco, California, Proceedings, p. 2.1–2.6.
- Freeman, A., Werner, C., and Klein, J. D., 1989, Results of the 1988 NASA/JPL Airborne SAR calibration campaign: *International Geoscience and Remote Sensing Symposium*, Vancouver, British Columbia, Proceedings, p. 249–253.
- Friedman, J. D., 1966, Composition of basalt flows at Pisgah Crater, California: Preliminary data: *NASA Technical Letter NASA-20*, 29 p.
- Fung, A. K., and Eom, H. J., 1979, Multiple scattering and depolarization by a randomly rough Kirchhoff surface: *IEEE Transactions on Antennas and Propagation*, v. 29, p. 463–471.
- Gaddis, L. R., and Greeley, R., 1990, Volcanism in NW Ishtar Terra, Venus: *Icarus*, v. 87, p. 327–338.
- Gaddis, L., Mougins-Mark, P., Singer, R., and Kaupp, V., 1989, Geologic analyses of Shuttle Imaging Radar (SIR-B) data of Kilauea Volcano, Hawaii: *Geological Society of America Bulletin*, v. 101, p. 317–332.
- Gaddis, L. R., Mougins-Mark, P. J., and Hayashi, J. N., 1990, Lava flow surface textures: SIR-B image texture, field observations, and terrain measurements: *Photogrammetric Engineering and Remote Sensing*, v. 56, p. 211–224.
- Gawarecki, S. J., 1964, Geologic reconnaissance report of the Pisgah Crater, California area: *NASA Technical Letter NASA-2*, 12 p.
- Glanzner, A. F., Farmer, G. L., Hughes, W. T., Wooden, J. L., and Pickthorn, W., 1991, Contamination of basaltic magma by mafic crust at Amboy and Pisgah craters, Mojave Desert, California: *Journal of Geophysical Research*, v. 96, p. 13673–13691.
- Head, J. W., Campbell, D. B., Elachi, C., Guest, J. E., McKenzie, D. P., Saunders, R. S., Schaber, G. S., and Schubert, G., 1991, Venus volcanism: Initial analysis from Magellan data: *Science*, v. 252, p. 276–288.
- Hess, P. C., and Head, J. W., 1990, Derivation of primary magmas and melting of crustal materials on Venus: Some preliminary petrogenetic considerations: *Earth, Moon, and Planets*, v. 50/51, p. 57–80.
- Huneycutt, B. L., 1989, The Spaceborne Imaging Radar (C): *IEEE Transactions on Geoscience and Remote Sensing*, v. 27, p. 164–169.
- Mougins-Mark, P. J., Pieri, D. C., Francis, P. W., Wilson, L., Self, S., Rose, W. I., and Wood, C. A., 1989, Remote sensing of volcanoes and volcanic terrains: *Eos (American Geophysical Union Transactions)*, v. 70, p. 1567–1575.
- Raney, R. K., 1984, Conceptual design of a satellite SAR: *International Geoscience and Remote Sensing Symposium*, Strasbourg, France, Proceedings, p. 801–807.
- Saunders, R. S., Pettengill, G. H., Arvidson, R. E., Sjogren, W. L., Johnson, W.T.K., and Pieri, L., 1990, The Magellan Venus Radar Mapping Mission: *Journal of Geophysical Research*, v. 95, p. 8339–8355.
- Schaber, G. G., Elachi, C., and Farr, T. G., 1980, Remote sensing data of SP mountain and SP lava flow in north-central Arizona: *Remote Sensing of Environment*, v. 9, p. 149–170.
- Theilig, E., Wall, S., and Saunders, R. S., 1989, Radar interpretation of lava fields as a function of incidence angle: Implications for interpretation of Magellan SAR data of Venus: *Lunar and Planetary Science Conference*, 19th, Proceedings, p. 323–333.
- Ulaby, F. T., Moore, R. K., and Fung, A. K., 1982, *Microwave remote sensing: Active and passive*. Volume 2. Radar remote sensing and surface scattering and emission theory: Reading, Massachusetts, Addison-Wesley, p. 816–880.
- Valenzuela, G. R., 1967, Depolarization of EM waves by slightly rough surfaces: *IEEE Transactions on Antennas and Propagation*, AP-15, p. 552–557.
- van Zyl, J. J., 1990, Calibration of polarimetric radar images using only image parameters and trihedral corner reflector responses: *IEEE Transactions on Geoscience and Remote Sensing*, v. 28, p. 337–348.
- van Zyl, J. J., Zebker, H. A., and Elachi, C., 1987, Imaging radar polarization signatures: Theory and observation: *Radio Science*, v. 22, p. 529–543.
- van Zyl, J. J., Burnette, C. F., and Farr, T. G., 1991, Inference of surface power spectra from inversion of multifrequency polarimetric radar data: *Geophysical Research Letters*, v. 18, p. 1787–1790.
- Wall, S., van Zyl, J. J., Arvidson, R. E., Theilig, E., and Saunders, R. S., 1988, The Mojave field experiment: Precursor to the planetary test site: *American Astronomical Society Bulletin*, v. 20, p. 809.
- Wall, S. D., Farr, T. G., Muller, J.-P., Lewis, P., and Leberl, F. W., 1991, Measurement of surface microtopography: *Photogrammetric Engineering and Remote Sensing*, v. 57, p. 1075–1078.
- Wise, W. S., 1966, Geologic map of the Pisgah and Sunshine Cone lava fields: *NASA Technical Letter*, NASA-11, 8 p.
- , 1969, Origin of basaltic magmas in the Mojave Desert area, California: *Contributions to Mineralogy and Petrology*, v. 23, p. 53–64.
- Zebker, H. A., van Zyl, J. J., and Held, D. N., 1987, Imaging radar polarimetry from wave synthesis: *Journal of Geophysical Research*, v. 92, p. 683–701.